International Journal of the Korean Society of Precision Engineering, Vol. 1, No. 1, June 2000.

Design and Strain Analysis of Precision 3-component Load Cell

Gab-Soon Kim* and Se-Hun Rhee**

*RIIT, Department of Control and Instrumentation Engineering, Gyeongsang National University, Chinju, South Korea
**Department of Precision Engineering, Hanyang University, Seoul, South Korea

ABSTRACT

This paper describes the development of a precision 3-component load cell with plate beams which may be used for measuring forces Fx, Fy and moment Mz simultaneously in industry. The equations to predict the bending strains on the surface of the beams under forces or moment are derived, the attachment location of strain gages of each sensor is determined, and 3-component load cell is fabricated. To evaluate the rated strain and interference error of each sensor, The characteristic test of precision 3-component load cell is carried out. It reveals that the rated strain calculated from the derived equations are good agreement with the results from Finite Element Method analysis.

Key Words: 3-component load cell, sensing element, force, moment, beam, strain, rated strain, finite element method, interference error, interference strain

Nomenclature

F_{Ax} : the force applied to the plate-beam A along the x-direction

F_{Ay} : the force applied to the plate-beam A along the y-direction

M_A : the moment applied to the plate-beam A

F_{Bx} : the force applied to the plate-beam B along the x-direction

F_{By} : the force applied to the plate-beam B along the y-direction

M_B : the moment applied to the plate-beam B

F_{Ey} : the force applied to the plate-beam E along the y-direction

M_E : the moment applied to the plate-beam E

F_{Gy} : the force applied to the plate-beam G along the y-direction

M_G : the moment applied to the plate-beam G

F_{Ix} : the force applied to the plate-beam I along the x-direction

F_{Iy} : the force applied to the plate-beam I along the y-direction

M_I : the moment applied to the plate-beam I

F_{Ky} : the force applied to the plate-beam K along the y-direction

F_{Ly} : the force applied to the plate-beam L along the y-direction

I : the moment of inertia of the area

Zp : the polar moment of inertia

E : the modulus of longitudinal elasticity

ε_{A-LF} : the strain produced on the left surface of plate-beam A

ε_{A-RI} : the strain produced on the right surface of plate-beam

ε_{B-LF} : the strain produced on the left surface of plate-beam B

ε_{B-RI} : the strain produced on the right surface of plate-beam B

ε_{E-U} : the strain produced on the upper surface of plate-beam E

ε_{E-L} : the strain produced on the lower surface of plate-beam E

ε_{G-U} : the strain produced on the upper surface of plate-beam G

ε_{G-L} : the strain produced on the lower surface of plate-beam G

ε_{I-U} : the strain produced on the upper surface of plate-beam I

ε_{I-L} : the strain produced on the lower surface of plate-beam I

ε_K : the strain produced on plate-beam K

ε_L : the strain produced on plate-beam L

1. Introduction

The multi-component load cell, which is a body that has more than two sensors of the load cells for measuring forces (Fx, Fy, Fz sensor) or load cells for measuring moments (Mx, My, Mz sensor), measures the forces Fx, Fy, Fz and the moments Mx, My, Mz which are applied to it simultaneously. The multi-component load cell is used in the automobile industry, shipbuilding industry, electronics industry, etc. for controlling the force of the robots and the machine tools, and also for measuring the forces and the moments. The multi-component load cell is fabricated by combining load cells which can detect the force and moment from each direction in one body. The 6-component load cell combines load cells which detect forces from three directions, Fx, Fy, Fz, and those which detect moments from three direction, Mx, My, Mz, into one body. A 2-component load cell combines 2 of the 6 load cells which detect forces or moments. A 3-component load cell combines 3 load cells, while a 4-component load cell combines 4 load cells, and a 5-component load cell combines 5 load cells. When measuring force and moment through a multi-component load cell, the multi-component load cell which can measure only the force and moment which is to be measured is selected. This is because of the high cost of the multi-component load cell. Therefore, in multi-component load cell manufacturing companies, 2-component~6-component load cells are individually designed, manufactured and patented.

The parallel plate(1~5) and radial plate(2,3) are widely used as a sensing element of the multi-component load cell. Kim(6) designed a 3-component load cell using the parallel plate structure. When the capacity is below 200 N, the structure of the 3-component load cell using the parallel plate structure is more complex than the multi-component load cell constructed from the plate, making manufacturing more difficult.

In addition, when the capacity is equal, more deflection is generated than the plate, making it impossible to be used in measuring high-precision forces and moments. Kim(7) used the plate beam to design a 6-component load cell. However, due to the inexperienced placement of the plate beam and the attachment location, the sensing element of the load cell could not be designed through an theory analysis. Instead, a trial and error process using the finite element method was used. In the case of a multi-component load cell with such a structure, the trial and error process through the finite element analysis is necessary to design a load cell with a different capacity of force and moment. Therefore, in order to construct the load cell of each direction efficiently and accurately, a theory analysis equation which can calculate the strain of the sensing element must be derived.

The precision accuracy of the multi-component load cell can be estimated by non-linearity, repeatability, and interference error. However, as the interference error is dozens or hundreds of times larger than the other errors, the precision accuracy of the multi-component load cell is estimated by the interference error. The interference error can be reduced by accurately locating the strain gauge, through design and strain analyzing the multi-component load cell sensing element.

In this paper, several plate beams were used to design an precision 3-component load cell which could detect the forces Fx, Fy and the moment Mx, simultaneously. Equations which calculate the strain of the beams according to the force and moment in order to design the sensing element of the load cell were derived, and these equations were used to design the size of the 3-component load cells sensing element. The reliability of the derived equations were verified by performing a finite element analysis of the

sensing element. The strain obtained through this process was compared to that obtained through the theory analysis. Also, the strains obtained from the theory analysis were used to determine the attachment location of the strain gauge, and the a full bridge circuit was formulated through the selected gauges to calculate the rated strain and interference error.

2. Theory analysis

2.1 Modeling of the sensing element

In this paper, plate-beams A~L were perpendicularly placed to detect forces Fx, Fy and moment Mz simultaneously. The sensing element of the precision 3-component load cell was modeled as shown in Fig. 1. The sensing element of the load cell which detects forces Fx and Fy was structured so that the plate-beams of the same size. Thus beams A~H which have a length of l_1, width of b_1, and height of h_1, were positioned in a square. The sensing element of the load cell which detects the moment Mz was structured so that the plate-beams of the same size, thus, beams I~L which have a length of l_2, width of b_2 and height of h_2, were positioned into a cross-shape, centering on the load transmitting block.

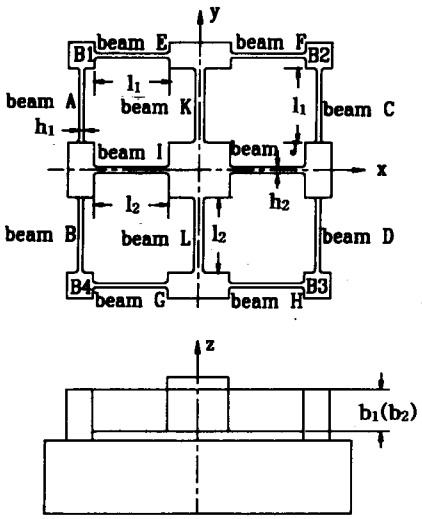

Fig. 1 Structure of sensing element for a precision 3-component load cell

Beam A~D , E~H, and I~L are the sensing elements for forces Fx, Fy and moment Mz, respectively. Blocks B1~B4 are used to fixate each beam to the body. The strain of each sensing element is used to design each load cell. Therefore, it is necessary to analyse the strain of the sensing element.

2.2 Theory analysis

2.2.1 Under force Fy

Beam A~D detect force Fx, and E~H detect force Fy. As shown in Fig. 1, beams A~L are placed symmetrically, centering on the load transmitting block. Therefore, a theoretical equation under force Fy is derived, the results of which are used when under force Fx. Fig. 2 shows the force and moment generated from each beam under Fy=P in the y-direction.

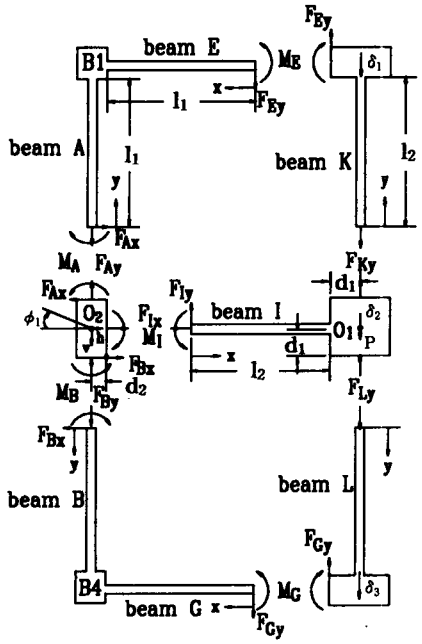

Fig. 2 Free body diagram of plate beams for a precision 3-component load cell under the force Fy

As a symmetry is formed centering on the central line under force P, the beams on the left are used to derive a theoretical equation, the results of which are used on the beams on the right. Under force P, the load transmitting block was deflected to δ_2, and

beams E and G to δ_1 and δ_3, respectively, in the direction in which the load is being applied, as shown in Fig. 2. The block between beams A, B and I rotate as much as ϕ_1.

By using the force and moment equilibrium condition of the blocks between the load transmitting block and beams A, B, and I, the following equations can be obtained

$$2F_{Ky}+2F_{Iy}=P \tag{1}$$

$$-F_{Ax}+F_{Ix}+F_{Bx}=0 \tag{2}$$

$$F_{Ay}+F_{By}-F_{Iy}=0 \tag{3}$$

$$M_I-M_A-M_B+d_2F_{Iy}-d_1F_{Ax}-d_1F_{Bx}=0 \tag{4}$$

The force equations and the moment equations are derived from the plate-beams. By substituting the derived equations into equation (2), the horizontal displacement h is 0. Also, by substituting the force equations and the moment equations into the equation (1), (3) and (4), the equations can be obtained as

$$k_{11}\delta_2+k_{12}v+k_{13}\phi_1=P \tag{5}$$

$$k_{14}\delta_2+k_{15}v+k_{16}\phi_1=0 \tag{6}$$

$$k_{17}\delta_2+k_{18}v+k_{19}\phi_1=0 \tag{7}$$

where, k11~k19 are coefficients, as shown in the following:

$$k_{11}=\frac{2A_2E}{l_2}\times\frac{1}{(1+\frac{A_2l_1^3}{24I_1l_2})}+\frac{24EI_2}{l_2^3}$$

$$k_{12}=-\frac{24EI_2}{l_2^3},$$

$$k_{13}=-\frac{24EI_2}{l_2^3}(d_2+\frac{l_2}{2})$$

$$k_{14}=-\frac{12EI_2}{l_2^3},\ k_{15}=\frac{2A_1E}{l_1}+\frac{12EI_2}{l_2^3}$$

$$k_{16}=\frac{12EI_2}{l_2^3}(d_2+\frac{l_2}{2})$$

$$k_{17}=\frac{6EI_2}{l_2^3}(2d_2+l_2) \tag{8}$$

$$k_{18}=-\frac{6EI_2}{l_2^3}(2d_2+l_2)$$

$$k_{19}=-\frac{12EI_2}{l_2^3}(d_2^2+d_2l_2+\frac{l_2^2}{3})-\frac{12EI_1}{l_1^3}(d_1^2+d_1l_1+\frac{l_1^2}{3})$$

The equations for analyzing the rated strains on the surfaces of the plate-beams E, G are derived by using the bending strain, which can be written as

$$\varepsilon_{E-U}=-\varepsilon_{E-L}=\varepsilon_{G-U}=-\varepsilon_{G-L}=\frac{A_2h_1\delta_2}{8I_1l_2}\times\frac{1}{1+\frac{A_2l_1^3}{24I_1l_2}}(l_2-2x) \tag{9}$$

The equations for analyzing the interference strains on the surfaces of the plate-beams A, B, I, K and L are derived by combining the bending strain and the tension or compression strain, which can be written as

$$\varepsilon_{I-U,L}=\frac{6h_2}{l_2^3}\left[\left\{\frac{\delta_2}{2}-\frac{v}{2}-(\frac{d_2}{2}+\frac{l_2}{3})\phi_1\right\}l_2-\left\{\delta_2-v-(d_2+\frac{l_2}{2})\phi_1\right\}x\right] \tag{10}$$

$$\varepsilon_{A-LF}=-\frac{6h_1}{l_1^3}\left[\left\{(\frac{d_1}{2}+\frac{l_1}{3})\phi_1\right\}l_1-\left\{(d_1+\frac{l_1}{2})\phi_1\right\}x\right]+\frac{v}{l_1} \tag{11}$$

$$\varepsilon_{A-RI}=\frac{6h_1}{l_1^3}\left[\left\{(\frac{d_1}{2}+\frac{l_1}{3})\phi_1\right\}l_1-\left\{(d_1+\frac{l_1}{2})\phi_1\right\}x\right]+\frac{v}{l_1} \tag{12}$$

$$\varepsilon_{B-LF}=\frac{6h_1}{l_1^3}\left[\left\{(\frac{d_1}{2}+\frac{l_1}{3})\phi_1\right\}l_1-\left\{(d_1+\frac{l_1}{2})\phi_1\right\}x\right]-\frac{v}{l_1} \tag{13}$$

$$\varepsilon_{B-RI}=-\frac{6h_1}{l_1^3}\left[\left\{(\frac{d_1}{2}+\frac{l_1}{3})\phi_1\right\}l_1-\left\{(d_1+\frac{l_1}{2})\phi_1\right\}x\right]-\frac{v}{l_1} \tag{14}$$

$$\varepsilon_K=-\varepsilon_L=\frac{\delta_2}{l_2(1+\frac{A_2l_1^3}{24I_1l_2})} \tag{15}$$

It is possible to calculate the strain of each beam under force Fy, by substituting the solution of equations (5)~(7), thus δ_2, v_1 and ϕ_1, to equations (9)~(15). Equation (9) is used to calculate the rated strain of the sensing element, and equations (10)~(15) are used into calculate the interference strain.

2.2.2 Under moment Mz

Beams I~L detect moment Mz. As shown in Fig.

1, beams A, B and I on the left, C, D and J on the right, E, F and K on the top, and G, H and L on the bottom are of the same size, centering on the load transmitting block. Therefore, the theoretical equation of beams A, B and I on the left is derived, and the results are applied to the other beams. Fig. 3 shows the force and moment generated from each beam under moment Mz=T/4 in the z-direction. As shown in Fig. 4, the load transmitting block and the block between beams A, B and I rotate as much as θ 2 and ψ 2, respectively, under moment Mz=T/4 in the z-direction.

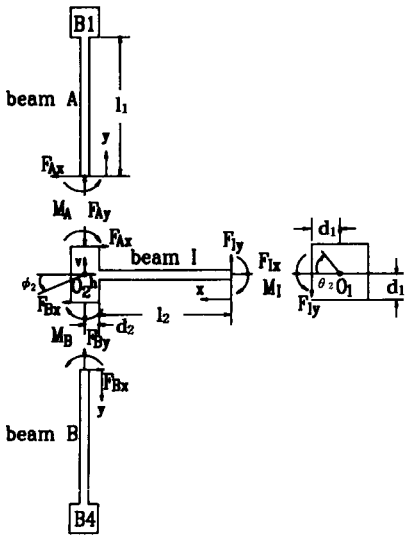

Fig. 3 Free body diagram of plate beams for a precision 3-component load cell under the moment Mz

By using the load transmitting block and the force and moment equilibrium condition of the x and y-directions of the block between beams A, B and I, The equations can be obtained

$$M_I + d_2 F_{Iy} = \frac{T}{4} \tag{16}$$

$$F_{Ax} + F_{Ix} - F_{Bx} = 0 \tag{17}$$

$$F_{Iy} - F_{Ay} - F_{By} = 0 \tag{18}$$

$$M_I + M_A + M_B - (d_2 + l_2)F_{Iy} + d_1 F_{Ax} + d_1 F_{Bx} = 0 \tag{19}$$

The force equations and the moment equations are derived from the plate-beams. Substituting the derived equations into the equation (17), the horizontal displacement h is 0. Also, by substituting the force equations and the moment equations into the equation (16), (18) and (19), the following equations can be obtained

$$k_{21}\theta_2 + k_{22}v + k_{23}\phi_2 = \frac{T}{4} \tag{20}$$

$$k_{24}\theta_2 + k_{25}v + k_{26}\phi_2 = 0 \tag{21}$$

$$k_{27}\theta_2 + k_{28}v + k_{29}\phi_2 = 0 \tag{22}$$

where, k21~k29 are coefficients, as shown in the following:

$$\begin{aligned}
k_{21} &= \frac{12EI_2}{l_2^3}\left(d_1^2 + d_1 l_2 + \frac{l_2^2}{3}\right) \\
k_{22} &= -\frac{24EI_2}{l_2^3}\left(d_1 + \frac{l_2}{2}\right) \\
k_{23} &= -\frac{24EI_2}{l_2^3}\left(\frac{d_2 l_2}{2} + \frac{l_2^2}{3} + d_1 d_2 + \frac{d_1 l_2}{2}\right) \\
k_{24} &= \frac{12EI_2}{l_2^3}\left(d_1 + \frac{l_2}{2}\right) \\
k_{25} &= -\frac{2A_1 E}{l_1} - \frac{12EI_2}{l_2^3} \\
k_{26} &= -\frac{12EI_2}{l_2^3}\left(d_2 + \frac{l_2}{2}\right) \\
k_{27} &= -\frac{12EI_2}{l_2^3}\left(\frac{d_1 l_2}{2} + d_1 d_2 + \frac{d_2 l_2}{2} + \frac{l_2^2}{6}\right) \\
k_{28} &= \frac{12EI_2}{l_2^3}\left(d_2 + \frac{l_2}{2}\right) \\
k_{29} &= \frac{12EI_2}{l_2^3}\left(d_2^2 + d_2 l_2 + \frac{l_2^2}{6}\right) \\
&\quad + \frac{24EI_1}{l_1^3}\left(d_1^2 + d_1 l_1 + \frac{l_1^2}{3}\right)
\end{aligned} \tag{23}$$

The equations for analyzing the rated strains on the surfaces of the plate-beam I are derived by using the bending strain, which can be written as

$$\varepsilon_{I-U} = \frac{6h_2}{l_2^3}\left[\left\{\left(\frac{d_1}{2} + \frac{l_2}{3}\right)\theta_2 - \frac{v}{2} - \left(\frac{d_2}{2} + \frac{l_2}{3}\right)\phi_2\right\} l_2 - \left\{\left(d_1 + \frac{l_2}{2}\right)\theta_2 - v - \left(d_2 + \frac{l_2}{2}\right)\phi_2\right\} x\right] \tag{24}$$

The equations for analyzing the interference strains on the surfaces of the plate-beams A and B are derived by combining the bending strain and the tension or the compression strain, which can be written as

$$\varepsilon_{A-LF} = \frac{6h_1}{l_1^3}\left[\left\{\left(\frac{d_1}{2}+\frac{l_1}{3}\right)\phi_2\right\}l_1 - \left\{\left(d_1+\frac{l_1}{2}\right)\phi_2\right\}x\right] - \frac{v}{l_1} \quad (25)$$

When the solutions θ_2, v, and ϕ_2 of the simultaneous equations of (20)~(22) are found and substituted into equations (24)~(28), the strain generated from each beam under moment Mz can be found.

$$\varepsilon_{A-RI} = -\frac{6h_1}{l_1^3}\left[\left\{\left(\frac{d_1}{2}+\frac{l_1}{3}\right)\phi_2\right\}l_1 - \left\{\left(d_1+\frac{l_1}{2}\right)\phi_2\right\}x\right] - \frac{v}{l_1} \quad (26)$$

$$\varepsilon_{B-LF} = -\frac{6h_1}{l_1^3}\left[\left\{\left(\frac{d_1}{2}+\frac{l_1}{3}\right)\phi_2\right\}l_1 - \left\{\left(d_1+\frac{l_1}{2}\right)\phi_2\right\}x\right] + \frac{v}{l_1} \quad (27)$$

$$\varepsilon_{B-RI} = \frac{6h_1}{l_1^3}\left[\left\{\left(\frac{d_1}{2}+\frac{l_1}{3}\right)\phi_2\right\}l_1 - \left\{\left(d_1+\frac{l_1}{2}\right)\phi_2\right\}x\right] + \frac{v}{l_1} \quad (28)$$

Equation (24) is used to calculate the rated strain of the sensing element, and equations (25)~(28) are used to calculate the interference strain.

3. The Sensing Element Design

The sensing element of the precision 3-component load cell must be designed so that under forces Fx, Fy and moment Mz, the strains output from the full bridge circuit of each load cell are similar to one another. The design variable is the attachment location under the consideration of the rated capacity, rated strain, width of beam, length of beam, and the size of the strain gauge. In order to design the sensing element, the rated capacity was determined at 100 N with forces Fx and Fy, and 2 Nm with moment Mz. The rated strain was approximately 1000 $\mu m/m$. Considering the size(4 × 5 mm^2), the attachment location of the strain gauge was determined at 3 mm from each end under forces Fx and Fy, and 5 mm from each end under moment Mz, in the length direction of the beam. The central line following the length of the beam was determined as the attachment location in the width direction of the beam.

The determined sizes were substituted into strain equations (9) and (24). The results of the calculation show that the length of the beam is l_1=l_2=17 mm, the height is h_1=1.4 mm, h_2=1.8 mm, and the width is b_1=b_2=14 mm. Aluminum 2024-T351, which is the most widely used material for small capacity load cell sensing elements, was used as material for the sensing element.

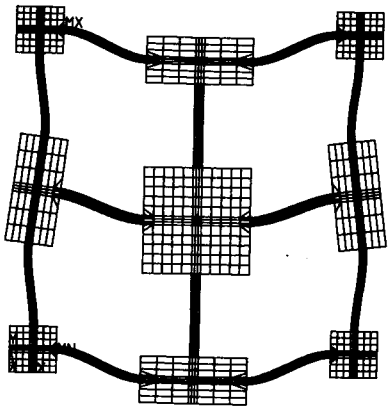

Fig. 4 Finite element mesh and deformed shape of beams for Fx, Fy, Mz load cell under the force Fx or Fy

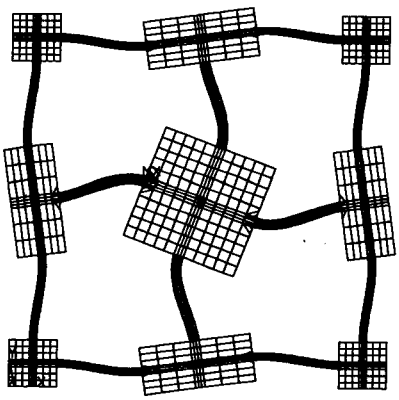

Fig. 5 Finite element mesh and deformed shape of beams for Fx, Fy, Mz load cell under the moment Mz

4. Finite element analysis

In order to confirm the strain calculated through the

theory analysis, the finite element analysis is performed on the sensing element of the load cell under force Fy and moment Mz. The finite element analysis uses ANSYS, which is a commercial finite element analysis program to calculate the strain on the beam in two dimensions. The analysis was hypothesized to be in a plan-stress state, and a 4 nodes element was used as the finite element. The material property was the modulus of longitudinal elasticity which is the constant value of the aluminum, thus 70 GPa, and the poisson's is 0.3. The mesh was in 0.5 mm intervals in the length direction of the beam, and the height was divided into three parts. In the finite element analysis, force Fy, 7.143 N/mm, which is the force per unit width of the beam, was applied in each y-direction.

A total of 14.6399 Nmm/mm was applied to the central location of the 4 bolts which fixate the load transmitting block and fixture jig(the location 9.758 mm from the center of the load transmitting block).

An enhanced version of the load cell sensing element's deformed shape is shown under force Fy in Fig. 4, and under moment Mz in Fig. 5. As hypothesized in the theory analysis, the deformed shape of the sensing element shows a right and left symmetry when force is applied, and a deformed behavior larger than the end of the fixture at a point close to the block when the moment is applied.

5. Results and Discussion of the strain analysis

Fig. 6~12 show the strain distribution generated from each beam when force Fy=100 N is applied to the load transmitting block. Fig. 6 and 7 show the force Fy load cell, thus, the strain distribution of beams E and G. Beams E and G have distributions of similar size. Also, both the theory analysis value and finite element increase and decrease linearly, with an absolute value strain, centering on the 8.5 mm point, which is the center of both ends of the beam. The theory analysis value and finite element analysis value coincide within a 6 % range in all areas excluding the 1 mm point from both ends of the beam. The finite element analysis value decreases at both ends because the end effect of the connecting point between the beam and the rigid body and the numerical error appear combinedly. Fig. 8~12 show the interference strain of each beam, A, B, I, K and L. Fig. 8 and 9 show the interference error of beams A and B, and the theory analysis value coincides with the finite element value, within 5 %. The theory analysis value and finite element analysis value are both 0 near the 9.5 mm point, because the block between beams A, B and I has rotated. The error rate of the finite element analysis value based on the theory analysis value coincides within 10 %, and shows a larger error rates from the theory analysis value as it nears the end of the beam. This is thought to be because although all blocks were hypothesized to be the rigid body during the theory analysis, they have minutely changed during the finite element analysis, disabling the force from being transferred. Fig. 11 and 12 show the interference strain of beams K and L. The error rate of the finite element value based on the theory analysis value coincides within 5 $\mu m/m$.

Fig. 13~15 show the strain of beams I, A and B when moment Mz=2 Nm is applied to the load transmitting block. Fig. 13 shows the strain of beam I, and the error rate of the finite element analysis value based on the theory analysis value shows a maximum of 13.6 %. This is thought to be because although all blocks were hypothesized to be the rigid body during the theory analysis, they have minutely changed during the finite element analysis, disabling the force from being transferred. Fig. 14 and 15 show the interference strain of beams A and B.

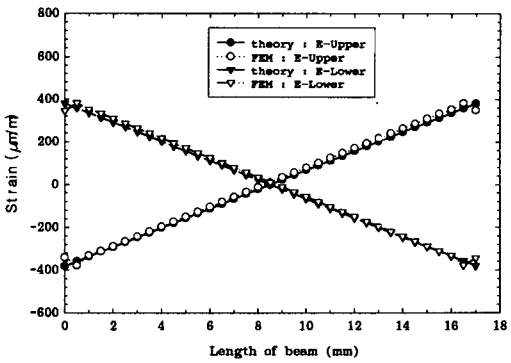

Fig. 6 Strain distribution of beam E under force Fy of -100 N

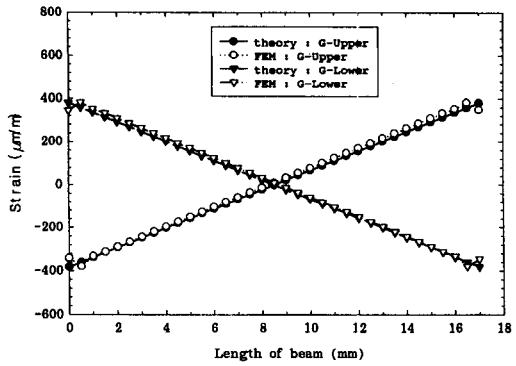

Fig. 7 Strain distribution of beam G under force Fy of -100 N

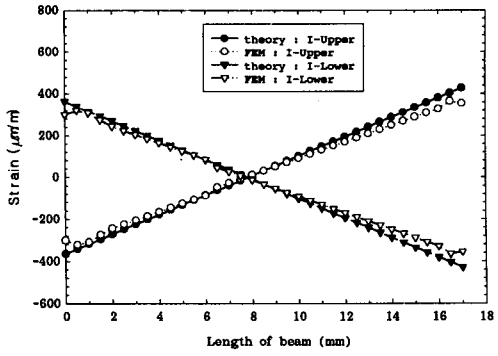

Fig. 10 Strain distribution of beam I under force Fy of -100 N

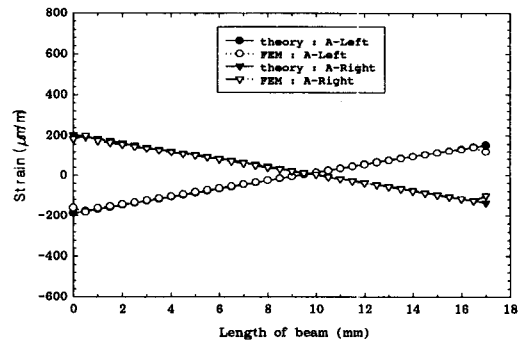

Fig. 8 Strain distribution of beam A under force Fy of -100 N

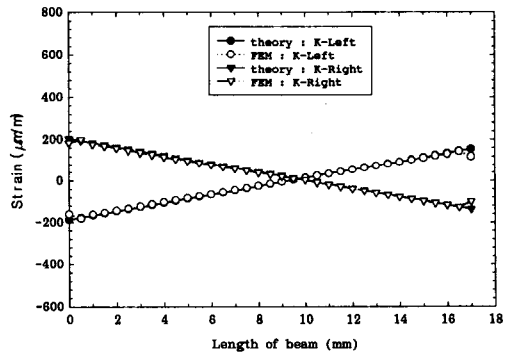

Fig. 11 Strain distribution of beam K under force Fy of -100 N

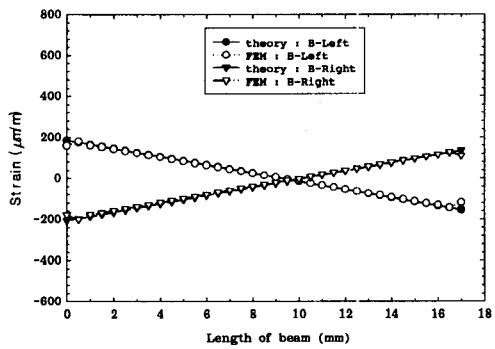

Fig. 9 Strain distribution of beam B under force Fy of -100 N

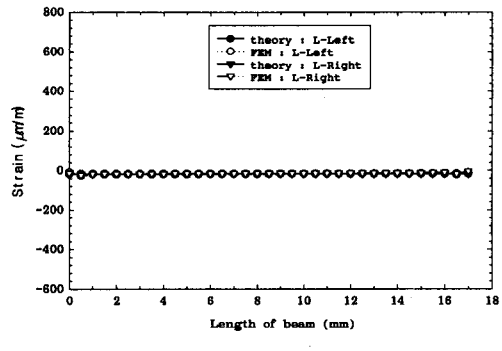

Fig. 12 Strain distribution of beam L under force Fy of -100 N

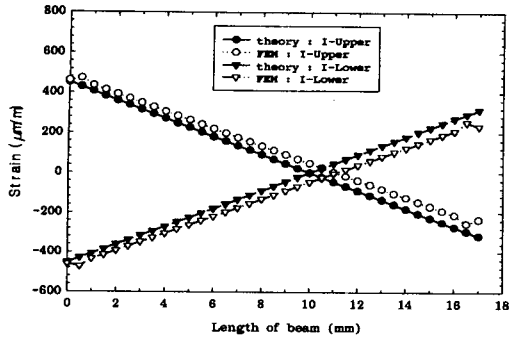

Fig. 13 Strain distribution of beam I under moment Mz of 2 Nm

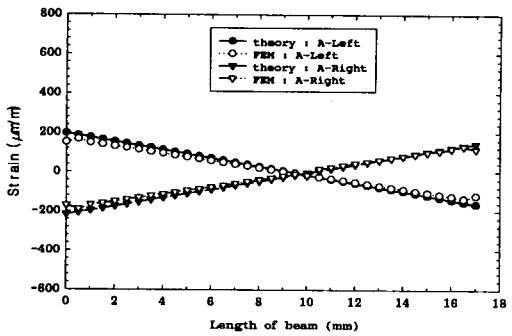

Fig. 14 Strain distribution of beam A under moment Mz of 2 Nm

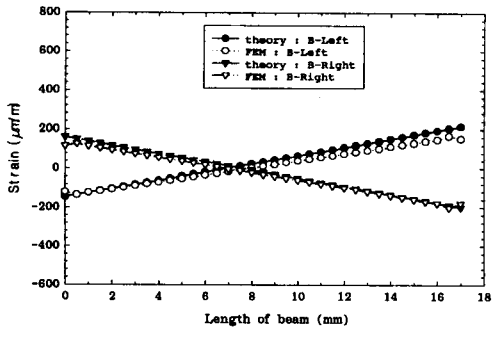

Fig. 15 Strain distribution of beam B under moment Mz of 2 Nm

The error rate of the finite element analysis value based on the theory analysis value coincides within a maximum of 11 %. The maximum error rate of 13.6 %, which is compared with the finite element value based on the theory analysis value, is thought to show satisfactory results, considering the analysis error of the analysis program. Therefore, it is judged that the strain equation derived in this paper is useful in the design of the precision 3-component load cell.

6. Calculation of rated strain and Interference error

Fig. 16 shows the locations where the strain gauges which detect each of the forces and moment can be attached. S1, S4, S5 and S8 are selected as the strain gauges for the load cell which detects forces Fx, S9, S12, S13 and S16 for the load cell which detects force Fy, and S33~S36 for the load cells which detect moment Mz.

The strain and interference strain of each attachment location of the load cell strain gauge is used to calculate the rated strain and interference error of each load cell through equation (28). The results are shown in Table 1.

$$\varepsilon = \varepsilon_{T1} - \varepsilon_{C1} + \varepsilon_{T2} - \varepsilon_{C2} \qquad (28)$$

where, ε is the strain calculated from the full bridge circuit, ε_{T1} is the strain of tension strain gauge T1, ε_{T2} is the strain of strain gauge T2, ε_{C1} is the strain of compression strain gauge C1, and ε_{C2} is the strain of compression strain gauge C2. The full bridge circuit is shown in Fig. 17.

In Table 1, the theory analysis value (rated strain) of Fx, Fy, Mz load cell are 984 $\mu m/m$, 984 $\mu m/m$, 1044 $\mu m/m$, the finite element analysis values are 968 $\mu m/m$, 968 $\mu m/m$, 1052 $\mu m/m$, and the experimental values are 956 $\mu m/m$, 1044 $\mu m/m$, 963 $\mu m/m$, and 1102 $\mu m/m$. As a result of comparing the finite element analysis based on the theory analysis, the rated strain error was found to be within 1.7 %, and the result of comparing the experimental values based on the theory analysis was 5.4 %. Also, the interference error which greatly affects the precision accuracy of the multi-component load cell was found to be 0 %, when the finite element analysis was compared based on the theory analysis.

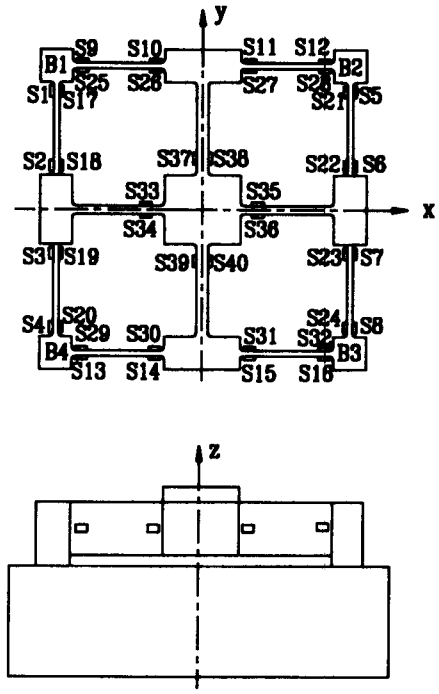

Fig. 16 Location of strain gages

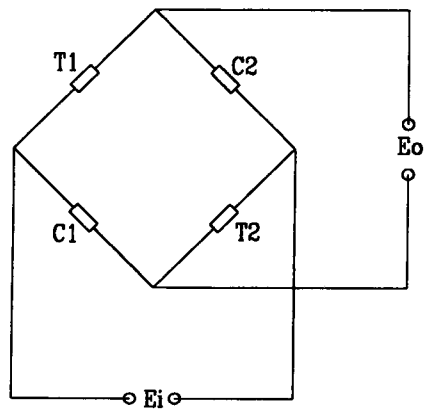

Fig. 17 Full bridge circuit

Therefore, equations (9) and (24) which were derived in this paper were judged to be useful in the rated strain for designing the precision 3-component load cell, and equations (10)~(15) and (25)~(27) were judged to be useful in calculating the interference strain. Also, the interference error of the precision 3-component load cell which was designed in both the theory analysis and finite element analysis was 0, confirming satisfactory results in the load cell manufacturing process.

Table. 1 Rated strain and interference error of each component

Load cell		Rated strain (μm/m)	Interference error (%)
Fx load cell	Theory	984	0
	FEM	968	0
	Experimental	956	1.0
Fy load cell	Theory	984	0
	FEM	968	0
	Experimental	963	1.5
Mz load cell	Theory	1044	0
	FEM	1052	0
	Experimental	1102	1.7

7. Conclusions

In this paper, the sensing element of the precision 3-component load cell was designed under force Fx=Fy=100 N and moment Mz=2 Nm. Several beams were combined to construct a precision 3-component load cell which could detect forces Fx, Fy and moment Mz simultaneously, and equations for calculating the strain of the beams due to the forces or moment were formulated, to design the sensing element of the load cell. The derived equations were used to design the size of the 3-component load cell sensing element, and a finite element analysis of the sensing element was performed, in order to confirm the reliability of the equations. The results are as follows.

(1) Based on the theory analysis, the rated strain error of the finite element analysis has a maximum value of within 1.7 %, and the result of the interference error is 0.

(2) Derived equations (9) and (24) are judged to be useful in the rated strain for designing the precision 3-component load cell, and equations (10)~(15) and (25)~(27) are judged to be useful in calculating the interference strain.

(3) The interference error of the precision 3-component load cell was 0 in both the finite element analysis and theory analysis, confirming satisfactory results in the load cell manufacturing process.

(4) The 3-component load cell designed in this paper can be used effectively for force control of the robot.

References

1. Yabuki, A., "Six-Axis Force/Torque Sensor for Assembly Robots," FUJTSU Sci. Tech. J., Vol. 26, No. 1, pp. 41~47, 1990.
2. Hatamura, Y., et al., "A Miniature 6-axis Force Sensor of Multilayer Parallel Plate Structure," IMEKO, pp. 567~582, 1989.
3. Ono, K., et. al., "A New Design for 6-component Force/Torque Sensors," Mechanical Problems in Measuring Force and Mass, pp. 39~48, 1993.
4. Ferrero, C., "The measurement of parasitic components in national force standard machines," Measurement Vol. 8 No. 2, pp. 66~76, 1990.
5. Jin-Won Joo, et. al., "Two-Axis Force Transducer for Measuring Flange Reaction Forces in the Tape Transport of VCR," Journal of KSME(A), Vol. 20, No. 7, pp. 2213~2222, 1996.
6. Gab-Soon Kim, et. al., "Design of Sensing Element for 3-component Load Cell Using Parallel Plate Structure," Journal of KSME(A), Vol. 21, No. 11, pp. 1871~1884, 1995.
7. Gab-Soon Kim, et. al., "Development of 6-component Load Cell Using Plate Beams," Journal of KSPE, Vol. 15, No. 8, pp. 109~115, 1998.
8. Gab-Soon Kim, et. al., "Standard Calibration Procedure of Electric Force Measuring Device (KASTO 97-07-104-104)," KASTO, pp. 3~15, 1997.